

[Fe(Phen)(CN)₄][−]: A Versatile Building Block for the Design of Heterometallic Systems. Crystal Structures and Magnetic Properties of PPh₄[Fe(Phen)(CN)₄]·2H₂O and [Fe(Phen)(CN)₄]₂M(H₂O)₂·4H₂O [Phen = 1,10-Phenanthroline; M = Mn(II) and Zn(II)]

Rodrigue Lescouëzec,^{1a} Francesc Lloret,^{1a} Miguel Julve,^{*,1a} Jacqueline Vaissermann,^{1b} Michel Verdaguer,^{*,1b} Rosa Llusar,^{1c} and Santiago Uriel^{1c}

Departament de Química Inorgànica, Facultat de Química de la Universitat de València, Dr. Moliner 50, 46100-Burjassot (València), Spain, Laboratoire de Chimie Inorganique et Matériaux Moléculaires, Unité CNRS 7071, Université Pierre et Marie Curie, 4 Place Jussieu, Case 42, 75252 Paris Cedex 05, France, and Departament de Ciències Experimentals, Campus Riu Sec de la Universitat Jaume I, POB 224, 12080 Castelló, Spain

Received November 8, 2000

The mononuclear PPh₄[Fe(phen)(CN)₄]·2H₂O (**1**) complex and the cyanide-bridged bimetallic [Fe(phen)(CN)₄]₂M(H₂O)₂·4H₂O compounds [M = Mn(II) (**2**) and Zn(II) (**3**); phen = 1,10-phenanthroline; PPh₄ = tetraphenylphosphonium cation] have been synthesized and structurally and magnetically characterized. Complex **1** crystallizes in the monoclinic system, space group *P*₂₁/*c*, with *a* = 9.364(4) Å, *b* = 27.472(5) Å, *c* = 14.301(3) Å, β = 97.68(2)°, and *Z* = 4. Complexes **2** and **3** are isostructural and they crystallize in the monoclinic system, space group *P*₂₁/*n*, with *a* = 7.5292(4) Å, *b* = 15.6000(10) Å, *c* = 15.4081(9) Å, β = 93.552(2)°, and *Z* = 2 for **2** and *a* = 7.440(1) Å, *b* = 15.569(3) Å, *c* = 15.344(6) Å, β = 93.63(2)°, and *Z* = 2 for **3**. The structure of complex **1** is made up of mononuclear [Fe(phen)(CN)₄][−] anions, tetraphenylphosphonium cations, and water molecules of crystallization. The iron(III) is hexacoordinate with two nitrogen atoms of a chelating phen (2.018(6) and 2.021(6) Å for Fe–N) and four carbon atoms of four terminal cyanide groups (Fe–C bond lengths varying in the range 1.906(8)–1.95(1) Å) building a distorted octahedron around the metal atom. The structure of complexes **2** and **3** consists of neutral double zigzag chains of formula [Fe(phen)(CN)₄]₂M(H₂O)₂ and crystallization water molecules. The [Fe(phen)(CN)₄][−] entity of **1** is present in **2** and **3** acting as a bridging ligand toward M(H₂O)₂ units [M = Mn(II) (**2**) and Zn(II) (**3**)] through two cyanide groups in cis positions, the other two cyanide remaining terminal. Two water molecules in trans positions and four cyanide-nitrogen atoms from four [Fe(phen)(CN)₄][−] units build a distorted octahedral surrounding Mn(II) (**2**) and Zn(II) (**3**). The M–O bond lengths are 2.185(3) Å (**2**) and 2.105(3) Å (**3**), whereas the M–N bond distances vary in the ranges 2.210(3)–2.258(3) Å (**2**) and 2.112(3)–2.186(3) Å (**3**). The structure of the [Fe(phen)(CN)₄][−] complex ligand in **2** and **3** is as in **1**. The shorter intrachain Fe–M distances through bridging cyano are 5.245(5) and 5.208(5) Å in **2** and 5.187(1) and 5.132(1) Å in **3**. The magnetic properties of **1–3** have been investigated in the temperature range 2.0–300 K. Complex **1** is a low-spin iron(III) complex with an appreciable orbital contribution. The magnetic properties of **3** correspond to the sum of two magnetically isolated spin triplets, the magnetic coupling between the low-spin iron(III) centers through the –CN–Zn–NC– bridging skeleton (iron–iron separation larger than 10.2 Å) being negligible. More interestingly, **2** exhibits one-dimensional ferrimagnetic behavior due to the noncompensation of the local interacting spins (*S*_{Mn} = 5/2 and *S*_{Fe} = 1/2) which interact antiferromagnetically through bridging cyano groups. A comparison between the magnetic properties of the isostructural compounds **2** and **3** allow us to check the antiferromagnetic coupling in **2**.

Introduction

An enormous amount of research work has been devoted to the study of cyanide-containing metal complexes because of their structural richness, unique spectroscopic properties, peculiar reactivity, and biological relevance.^{2,3} Restricting ourselves to their electronic aspects, topics such as the achievement of molecular-based magnets where the value of *T*_c can be tuned^{4–8}

and the design of high nuclearity clusters with tunable high spins and anisotropy^{9–11} have known spectacular results in the past decade. The synthetic strategy which is used to prepare these systems consists of reacting stable hexacyanometalate complexes of formula [B(CN)₆]^{q−} with either totally hydrated metal ions [A(H₂O)₆]^{p+} or partially blocked [A(L)_x(H₂O)_y]^{p+} species (A and B are transition metal ions and L is a polydentate ligand). In the first case, the Prussian blue Fe₄[Fe(CN)₆]₃·*n*H₂O (*T*_c = 5.5 K)¹² and Prussian blue analogues of formula A_q[B(CN)₆]_p·*n*H₂O and C_{q−p}A[B(CN)₆]_p·*n*H₂O (C is a monovalent cation) are obtained. This family of compounds exhibits a highly symmetrical three-dimensional network with the hexacyanometalate [B(CN)₆]^{q−} units describing a face-centered cubic motif and the

* To whom correspondence should be addressed.

- (1) (a) Universitat de València. (b) Université Pierre et Marie Curie. (c) Universitat Jaume I.
 (2) Dunbar, K. M.; Heintz, R. A. *Prog. Inorg. Chem.* **1997**, *45*, 283 and references therein.
 (3) Fehlhammer, W. P.; Fritz, M. *Chem. Rev.* **1993**, *93*, 1243 and references therein.

A cations in octahedral sites linking them.^{13–15} The A/B ratio can be varied depending on the charges on the metal ions A and B and on the insertion of cations (C) in part of the tetrahedral sites of the cubic structure. However, the progress concerning the analysis and comprehension of the highly interesting magnetostuctural results of these materials is conditioned by the fact that structural knowledge for the Prussian blue family is still limited and also by the lack of suitable models to analyze the magnetic properties of three-dimensional systems. The need for a better fundamental knowledge of these high- T_c cyano-bridged systems led the preparative chemist to replace the fully hydrated $[A(H_2O)_6]^{p+}$ species with the coordinatively unsaturated $[A(L)_x(H_2O)_y]^{p+}$ one.¹⁶ This approach has been highly rewarding. Limiting ourselves for brevity reasons to the results obtained when B = Fe(III), new bimetallic chain,¹⁷ layered,¹⁸ and three-dimensional¹⁹ compounds and even the ionic

$K[Cu(en)_2][Fe(CN)_6]$ salt²⁰ (en = ethylenediamine) have been reported recently. These results indicate that the presence of capping ligands in the coordination sphere of the A metal ion should be combined with a more specifically tailored hexacyano-metalate unit to direct the synthetic process toward the formation of discrete polynuclear species.

To investigate the structure and magnetic properties of low-dimensionality bimetallic cyano-bridged compounds, we have undertaken a new synthetic approach based on the use of the ligand-substituted cyano complex $[B^{III}(L)_x(CN)_y]^{(0-3)-}$ (L = polydentate ligand) as ligand toward transition metal ions. Our first results with B = Fe(III), L = 1,10-phenanthroline, and A = Mn(II) and Zn(II) allowed us to prepare the mononuclear precursor $PPh_4[Fe(phen)(CN)_4] \cdot 2H_2O$ (**1**) (PPh_4 = tetraphenylphosphonium cation) and the isostructural bimetallic compounds $\{[Fe(phen)(CN)_4]_2M(H_2O)_2\} \cdot 4H_2O$ with M = Mn(II) (**2**) and Zn(II) (**3**). Their preparation, crystal structure, and magnetic properties are presented.

Experimental Section

Materials. Chemicals were purchased from standard sources and used as received. $K_2[Fe(phen)(CN)_4] \cdot 4H_2O$ was prepared as described in the literature.²¹ Elemental analysis (C, H, N) was performed by the Microanalytical Service of the Universidad Autónoma de Madrid. The values of the Fe/P (**1**), Fe/Mn (**2**), and Fe/Zn (**3**) molar ratios (1:1 (**1**) and 2:1 (**2** and **3**)) were determined by electron microscopy at the Servei de Microscopia Electrònica de la Universitat de València.

Syntheses. $PPh_4[Fe(phen)(CN)_4] \cdot 2H_2O$ (1**).** Chlorine gas was passed into a warm dark red aqueous solution of $K_2[Fe(phen)(CN)_4] \cdot 4H_2O$ (4 mmol, 200 mL) under continuous stirring. After half an hour, the solution was filtered and the small amount of insoluble product was discarded. The addition of a concentrated warm aqueous solution of tetraphenylphosphonium chloride (4 mmol, 30 mL) causes the precipitation of complex **1** as an orange solid. Recrystallization in acetonitrile affords parallelepiped orange crystals of **1** which are of X-ray quality. The yield is about 90%. Anal. Calcd for $C_{40}H_{32}FePN_6O_2$ (**1**): C, 67.15; H, 4.48; N, 11.75. Found: C, 66.86; H, 4.54; N, 11.75.

$\{[Fe(phen)(CN)_4]_2M(H_2O)_2\} \cdot 4H_2O$ with M = Mn (2**) and Zn (**3**).** The synthetic procedure for complexes **2** and **3** is the same, the difference being the nature of the starting perchlorate salt. The preparation of complex **2** (**3**) is as follows: manganese(II) (zinc(II)) perchlorate hexahydrate dissolved in a minimum amount of methanol (0.1 mmol, 5 mL) is added to a methanolic solution of complex **1** (0.2 mmol, 25 mL). The red (orange) precipitate formed immediately is filtered off and washed thoroughly with acetonitrile to remove the tetraphenylphosphonium perchlorate salt. Red (**2**) and orange (**3**) prisms were obtained by recrystallization of the remaining solid in warm water. They were suitable for X-ray diffraction. The yield is about 15%. The yield is much improved (more than 90%) by using the lithium derivative of **1** as starting cyano-containing salt and water as solvent. Anal. Calcd for $C_{32}H_{28}Fe_2MnN_{12}O_6$ (**2**): C, 45.57; H, 3.32; N, 19.94. Found: C, 45.24; H, 3.28; N, 19.95. Anal. Calcd for $C_{32}H_{28}Fe_2ZnN_{12}O_6$ (**3**): C, 45.02; H, 3.28; N, 19.70. Found: C, 44.83; H, 3.20; N, 19.59.

Physical Measurements. The IR spectra (KBr pellets) were recorded with a Bruker IF S55 spectrophotometer. Magnetic susceptibility measurements (2.0–300 K) under an applied field of 0.1 T were carried out with a Quantum Design SQUID magnetometer. Diamagnetic

- (4) (a) Verdager, M.; Bleuzen, A.; Marvaud, V.; Vaissermann, J.; Seuleiman, M.; Desplanches, C.; Scuille, A.; Train, C.; Garde, R.; Gelly, G.; Lomenech, C.; Rosenman, I.; Veillet, R.; Cartier, C.; Villain, F. *Coord. Chem. Rev.* **1999**, *190–192*, 1023. (b) Garde, R.; Desplanches, C.; Bleuzen, A.; Veillet, P.; Verdager, M. *Mol. Cryst. Liq. Cryst.* **1999**, *334*, 587. (c) Ferlay, S.; Mallah, T.; Ouahès, R.; Veillet, P.; Verdager, M. *Inorg. Chem.* **1999**, *38*, 229. (d) Verdager, M.; Bleuzen, A.; Train, C.; Garde, R.; Fabrizzi de Viani, F.; Desplanches, C. *Philos. Trans. R. Soc. London, Ser. A* **1999**, *357*, 2959. (e) Dujardin, E.; Ferlay, S.; Phan, X.; Desplanches, C.; Cartier dit Moulin, C.; Sainctavit, P.; Baudet, F.; Dartyge, E.; Veillet, P.; Verdager, M. *J. Am. Chem. Soc.* **1998**, *120*, 11347. (f) Verdager, M. *Science* **1996**, *272*, 698. (g) Ferlay, S.; Mallah, T.; Ouahès, R.; Veillet, P.; Verdager, M. *Nature* **1995**, *378*, 701. (h) Mallah, T.; Thiébaud, S.; Verdager, M.; Veillet, P. *Science* **1993**, *262*, 1554. (i) Gadet, V.; Mallah, T.; Castro, I.; Veillet, P.; Verdager, M. *J. Am. Chem. Soc.* **1992**, *114*, 9213.
- (5) (a) Holmes, S. M.; Girolami, G. S. *J. Am. Chem. Soc.* **1999**, *121*, 5593. (b) Entley, W. R.; Treadway, C. R.; Wilson, S. R.; Girolami, G. S. *J. Am. Chem. Soc.* **1997**, *119*, 6251. (c) Entley, W. R.; Girolami, G. S. *Science* **1995**, *268*, 397. (d) Entley, W. R.; Treadway, C. R.; Girolami, G. S. *Mol. Cryst. Liq. Cryst.* **1994**, *273*, 153. (e) Entley, W. R.; Girolami, G. S. *Inorg. Chem.* **1994**, *33*, 5165.
- (6) (a) Sato, O.; Einaga, A.; Fujishima, A.; Hashimoto, K. *Inorg. Chem.* **1999**, *38*, 4405. (b) Sato, O.; Iyoda, T.; Fujishima, A.; Hashimoto, K. *Science* **1996**, *271*, 49.
- (7) Hatlevik, O.; Buchmann, W. E.; Zhang, J.; Manson, J. L.; Millere, J. S. *Adv. Mater.* **1999**, *11*, 914.
- (8) (a) Sra, A. K.; Andruh, M.; Kahn, O.; Golhen, S.; Ouahab, L.; Yakhmi, J. V. *Angew. Chem., Int. Ed.* **1999**, *38*, 2606. (b) Larionova, J.; Kahn, O.; Golhen, S.; Ouahab, L.; Clérac, R.; Bartolomé, J.; Burriel, R. *Mol. Cryst. Liq. Cryst.* **1999**, *334*, 651.
- (9) (a) In ref 4a, pp 1042–1044. (b) Mallah, T.; Marvilliers, A.; Rivière, E. *Philos. Trans. R. Soc. London, Ser. A* **1999**, *357*, 3139. (c) Mallah, T.; Auberger, C.; Verdager, M.; Veillet, P. *J. Chem. Soc., Chem. Commun.* **1995**, 61. (d) Scuille, A.; Mallah, T.; Nivorozhkin, A.; Tholence, J.-L.; Verdager, M.; Veillet, P. *New J. Chem.* **1996**, *20*, 1.
- (10) Langerberg, K. V.; Batten, S. R.; Berry, K. J.; Hockless, D. C. R.; Moubaraki, B.; Murray, K. S. *Inorg. Chem.* **1997**, *36*, 5006.
- (11) Marvilliers, A.; Pei, Y.; Cano Boquera, J.; Vostrikova, K. E.; Paulsen, C.; Rivière, E.; Audière, J.-P.; Mallah, T. *Chem. Commun.* **1999**, 1951.
- (12) Ito, A.; Suenaga, M.; Ono, K. *J. Chem. Phys.* **1968**, *48*, 3597.
- (13) Güdel, H. U.; Stucki, H.; Lüdi, A. *Inorg. Chim. Acta* **1973**, *7*, 121.
- (14) Lüdi, A.; Güdel, H. U. *Struct. Bonding (Berlin)* **1973**, *14*, 1.
- (15) In ref 2, pp 323–325.
- (16) Ohba, M.; Okawa, H. *Coord. Chem. Rev.* **2000**, *198*, 313 and references therein.
- (17) (a) Colacio, E.; Domínguez-Vera, J. M.; Ghazi, M.; Kivekäs, R.; Moreno, J. M.; Pajunen, A. *J. Chem. Soc., Dalton Trans.* **2000**, 505. (b) Eriksen, J. Ø.; Hazell, A.; Jensen, A.; Jepsen, J.; Poulsen, R. D. *Acta Crystallogr.* **2000**, *C56*, 551. (c) Colacio, E.; Domínguez-Vera, J. M.; Ghazi, M.; Kivekäs, R.; Klinga, M.; Moreno, J. M. *Chem. Commun.* **1998**, 1071. (d) Ohba, M.; Usuki, N.; Fukita, N.; Okawa, H. *Inorg. Chem.* **1998**, *37*, 3349. (e) Re, N.; Gallo, E.; Floriani, C.; Miyasaka, H.; Matsumoto, N. *Inorg. Chem.* **1996**, *35*, 6004. (f) Kou, H.-Z.; Liao, D.-Z.; Cheng, P.; Jiang, Z.-H.; Yan, S.-P.; Wang, G.-L.; Yao, X.-K.; Wang, H.-G. *J. Chem. Soc., Dalton Trans.* **1997**, 1503. (g) Fu, D. G.; Chen, J.; Tan, X. S.; Jiang, L. J.; Zhang, S. W.; Zheng, P. J.; Tang, W. X. *Inorg. Chem.* **1997**, *36*, 220. (h) Ohba, M.; Maruono, N.; Okawa, H. *J. Am. Chem. Soc.* **1994**, *116*, 11566. (i) Morpurgo, G. O.; Mosini, V.; Porta, P.; Dessy, G.; Fares, V. *J. Chem. Soc., Dalton Trans.* **1981**, 111.

- (18) (a) Smith, J. A.; Galán-Mascarós, J. R.; Clérac, R.; Dunbar, K. R. *Chem. Commun.* **2000**, 1077. (b) Colacio, E.; Domínguez-Vera, J. M.; Ghazi, M.; Kivekäs, R.; Lloret, F.; Moreno, J. M.; Stoeckli-Evans, H. *Chem. Commun.* **1999**, 987. (c) Ohba, M.; Fukita, N.; Okawa, H.; Hashimoto, Y. *J. Am. Chem. Soc.* **1997**, *119*, 1011. (d) Miyasaka, H.; Matsumoto, N.; Okawa, H.; Re, N.; Gallo, E.; Floriani, C. *Angew. Chem., Int. Ed. Engl.* **1995**, *34*, 1446.
- (19) El Fallah, M. S.; Rentschler, E.; Caneschi, A.; Sessoli, R.; Gatteschi, D. *Angew. Chem. Int. Ed. Engl.* **1996**, *35*, 1947.
- (20) Kang, B. S.; Tong, Y. X.; Yu, K. B.; Su, C. Y.; Zhang, H. X. *Acta Crystallogr.* **2000**, *C56*, 40.
- (21) Schilt, A. A. *J. Am. Chem. Soc.* **1960**, *82*, 3000.

Table 1. Crystallographic Data for PPh₄[Fe(phen)(CN)₄]⁻·2H₂O (**1**), [Fe(phen)(CN)₄]₂Mn(H₂O)₂·4H₂O (**2**), and [Fe(phen)(CN)₄]₂Zn(H₂O)₂·4H₂O (**3**)

compd	1	2	3
formula	C ₄₀ H ₃₂ FePN ₆ O ₂	C ₃₂ H ₂₈ Fe ₂ MnN ₁₂ O ₆	C ₃₂ H ₂₈ Fe ₂ ZnN ₁₂ O ₆
<i>f</i> _w	715.56	843.30	853.72
space group	<i>P</i> 2 ₁ / <i>c</i>	<i>P</i> 2 ₁ / <i>n</i>	<i>P</i> 2 ₁ / <i>n</i>
<i>a</i> , Å	9.364(4)	7.5292(4)	7.440(1)
<i>b</i> , Å	27.472(5)	15.6000(10)	15.569(3)
<i>c</i> , Å	14.301(3)	15.4081(9)	15.344(6)
β, deg	97.68(2)	93.552(2)	93.63(2)
<i>V</i> , Å ³	3646(2)	1806.29(18)	1773.7(9)
<i>Z</i>	4	2	2
λ, Å	0.71069	0.71073	0.71069
ρ _{calcd} , g cm ⁻³	1.30	1.55	1.60
<i>T</i> , °C	22	20	22
μ(Mo Kα), cm ⁻¹	4.96	11.98	15.5
<i>R</i> ^a	0.064	0.0402	0.0492
<i>R</i> _w ^b	0.076	0.0833	0.0608

^a $R = \sum(|F_o| - |F_c|) / \sum|F_o|$ for **1–3**. $R_w = [\sum w(|F_o| - |F_c|)^2 / \sum w F_o^2]^{1/2}$ for **1** and **3** and $R_w = [\sum w(|F_o|^2 - |F_c|^2) / \sum w F_o^2]^{1/2}$ for **2**; $w = w' [1 - (|F_o| - |F_c|) / 6\sigma(F_o)]^2$ for **1** and **3** with $w' = 1 / \sum A_i T_i(X)$ with three coefficients for a Chebyshev series (5.03, -0.168, and 3.80 for **1** and 4.54, 2.43, and 3.22 for **3**) for which $X = F_o / F_c(\max)$ and $w = 1 / [\sigma^2(F_o)^2 + (0.0408P)^2 + 0.0000P]$ for **2** where $P = (F_o^2 + 2F_c^2)/3$.

corrections of the constituent atoms were estimated from Pascal constants²² as -450×10^{-6} (**1**), -472×10^{-6} (**2**), and -473×10^{-6} (**3**) cm³ mol⁻¹.

X-ray Data Collection and Structure Refinement. Crystals of dimensions 0.30 mm × 0.35 mm × 0.50 mm (**1**), 0.18 mm × 0.15 mm × 0.07 mm (**2**), and 0.20 mm × 0.50 mm × 0.60 mm (**3**) were mounted on Enraf-Nonius CAD-4 (**1** and **3**) and Bruker Smart CCD (**2**) diffractometers and used for data collection. Diffraction data were collected at room temperature by using graphite-monochromated Mo Kα radiation [$\lambda = 0.71069$ (**1** and **3**) and 0.71073 Å (**2**)] with the ω - 2θ method. A nominal crystal to detector distance of 4.0 cm is used in the case of **2**. Accurate cell dimensions and orientation matrices (**1** and **3**) were obtained by least-squares refinements of 25 accurately centered reflections with $13.0^\circ < \theta < 13.5^\circ$ (**1**) and $12.9^\circ < \theta < 13.3^\circ$ (**3**). No significant variations were observed in the intensities of two checked reflections (**1–3**) during data collections. The data were corrected for Lorentz and polarization effects (**1–3**). An empirical absorption correction (**1** and **3**) was performed by the use of DIFABS.²³ A hemisphere of data (**2**) was collected based on three ω -scan runs (starting $\omega = 28^\circ$) at values of $\phi = 0^\circ, 90^\circ$, and 180° with the detector at $2\theta = 28^\circ$. At each of these runs, frames (606, 435, and 230, respectively) were collected at 0.3° intervals and 45 s per frame. The diffraction frames were integrated using the SAINT package²⁴ and corrected for absorption with SADABS.²⁵ Information concerning crystallographic data collections and structure refinements is summarized in Table 1. The maximum and minimum transmission factors were 1.00 and 0.93 for **1**, 0.97 and 0.78 for **2**, and 1.00 and 0.76 for **3**. Of the 6973 (**1**), 11 312 (**2**), and 4783 (**3**) measured reflections in the θ range $1-25^\circ$ (**1**), $1.86-26.37^\circ$ (**2**), and $1-28^\circ$ (**3**) with index ranges $0 \leq h \leq 11, 0 \leq k \leq 32$ and $-16 \leq l \leq 16$ (**1**), $-8 \leq h \leq 9, -19 \leq k \leq 17$ and $-17 \leq l \leq 19$ (**2**) and $0 \leq h \leq 9, 0 \leq k \leq 20$ and $-20 \leq l \leq 20$ (**3**), 6391 (**1**), 3699 (**2**), and 4257 (**3**) were unique. From these, 2411 (**1**), 2379 (**2**), and 2801 (**3**) were observed [$I > 3\sigma(I)$ (**1** and **3**) and $I > 2\sigma(I)$ (**2**)] and used for the refinement of the structures.

The structures of **1–3** were solved by direct methods through the SHELX-86 (**1** and **3**) and SHELXTL 5.10 (**2**) programs^{26,27} and

Table 2. Selected Bond Lengths (Å) and Angles (deg)^a for **1**

Fe(1)–N(5)	2.018(6)	Fe(1)–N(6)	2.021(6)
Fe(1)–C(1)	1.911(9)	Fe(1)–C(2)	1.906(8)
Fe(1)–C(3)	1.955(9)	Fe(1)–C(4)	1.95(1)
C(1)–N(1)	1.15(1)	C(2)–N(2)	1.15(1)
C(3)–N(3)	1.14(1)	C(4)–N(4)	1.14(1)
N(5)–Fe(1)–N(6)	81.0(2)	N(5)–Fe(1)–C(1)	177.1(3)
N(5)–Fe(1)–C(2)	93.5(3)	N(5)–Fe(1)–C(3)	91.8(3)
N(5)–Fe(1)–C(4)	91.2(3)	N(6)–Fe(1)–C(1)	96.2(3)
N(6)–Fe(1)–C(2)	174.3(3)	N(6)–Fe(1)–C(3)	90.8(3)
N(6)–Fe(1)–C(4)	92.1(3)	C(1)–Fe(1)–C(2)	89.3(3)
C(1)–Fe(1)–C(3)	87.4(3)	C(1)–Fe(1)–C(4)	89.7(4)
C(2)–Fe(1)–C(3)	88.1(3)	C(2)–Fe(1)–C(4)	89.3(3)
C(3)–Fe(1)–C(4)	176.1(3)	Fe(1)–C(1)–N(1)	177.0(8)
Fe(1)–C(2)–N(2)	176.3(8)	Fe(1)–C(3)–N(3)	175.6(7)
Fe(1)–C(4)–N(4)	179.3(8)		

^a Estimated standard deviations in the last significant digits are given in parentheses.

subsequently refined by Fourier recycling. The iron atom, the cyanide groups, and the non-hydrogen atoms of the phenanthroline ligand in **1** and all non-hydrogen atoms in **2** and **3** were refined anisotropically. Water oxygens and non-hydrogen atoms of the tetraphenylphosphonium cation in **1** were isotropically refined. One of the water molecules in **1** (O(2)) is disordered in two positions, each site being given occupancy factors of 0.4 and 0.6. The hydrogen atoms of the phenanthroline ligand in **1–3** and those of the water molecules in **3** were calculated and refined isotropically as riding atoms. The hydrogen atoms of the water molecules in **1** were neither found nor calculated, whereas those in **2** were found in a difference Fourier map and refined isotropically. The final full-matrix least-squares refinement on F (**1** and **3**) and F^2 (**2**) through the PC version of CRYSTALS²⁸ (**1** and **3**) and SHELXTL 5 × 10²⁷ (**2**) reached convergence with values of the *R* and *R*_w indices listed in Table 1, the number of variable being 322 (**1**), 265 (**2**), and 243 (**3**). The residual maxima and minima in the final Fourier-difference maps were 0.71 and $-0.34 \text{ e } \text{Å}^{-3}$ for **1**, 1.20 and $-0.27 \text{ e } \text{Å}^{-3}$ for **2**, and 0.63 and $-0.77 \text{ e } \text{Å}^{-3}$ for **3**. The values of the goodness-of-fit are 1.12 (**1**), 0.944 (**2**), and 1.02 (**3**). Selected interatomic bond distances and angles are given in Tables 2 (**1**), 3 (**2**), and 4 (**3**).

Results and Discussion

Description of the Structures. PPh₄[Fe(phen)(CN)₄]⁻·2H₂O (1**).** The structure of complex **1** consists of mononuclear [Fe(phen)(CN)₄]⁻ anions (Figure 1), tetraphenylphosphonium cations, and water molecules of crystallization which are linked by electrostatic forces, hydrogen bonds, and van der Waals interactions.

Each iron(III) cation is coordinated by two phen nitrogen and four cyanide carbon atoms, taking a distorted octahedral geometry. The short bite of chelating phen [82.08(11)° for N(5)–Fe(1)–N(6)] is one of the main factors accounting for this distortion. The values of the Fe(1)–N(phen) bonds in **1** [2.018(6) and 2.021(6) Å] are somewhat longer than that found in the low-spin iron(II) complexes [Fe(phen)₂(CN)₂] [1.966(4)–2.003(5) Å]²⁹ and [Fe(phen)₃](ClO₄)₂·¹/₂H₂O [1.965(8)–1.984(7) Å].³⁰ The Fe(1)–C(cyano) bond distances of **1** [1.906(8)–1.95(1)] are in good agreement with those reported for the low-spin iron(III) mononuclear complex [Fe(bpy)₂(CN)₂]-

- (22) Earnshaw, A. *Introduction to Magnetochemistry*; Academic Press: London, 1968.
 (23) Walker, N.; Stuart, D. *Acta Crystallogr.* **1983**, *A39*, 156.
 (24) SAINT, version 5.0; Bruker Analytical X-ray Systems: Madison, WI, 1998.
 (25) Sheldrick, G. M. *SADABS empirical absorption program*; University of Göttingen: Göttingen, Germany, 1996.

- (26) (a) Sheldrick, G. M. *SHELX-86: Program for Crystal Structure Solution*; University of Göttingen: Göttingen, Germany, 1986. (b) Watkin, D. J.; Prout, C. K.; Pearce, L. J. *Cameron*; Crystallography Laboratory, University of Oxford: Oxford, U.K., 1996.
 (27) SHELXTL, version 5.1; Bruker AXS, Inc.: Madison, WI, 1997.
 (28) Watkin, D. J.; Prout, C. K.; Carruthers, J. R.; Betteidge, P. W. *CRYSTALS*; Chemical Crystallography Laboratory, University of Oxford: Oxford, U.K., 1996; Issue 10.
 (29) Zhan, S.; Meng, Q.; You, X.; Wang, G.; Zheng, P. *J. Polyhedron* **1996**, *15*, 2665.
 (30) Koh, L. L.; Xu, Y.; Hsieh, A. K. *Acta Crystallogr.* **1994**, *C50*, 884.

Table 3. Selected Bond Lengths (Å) and Angles (deg)^{a,b} for **2**

Fe(1)–N(5)	1.992(2)	Fe(1)–N(6)	1.995(3)
Fe(1)–C(1)	1.922(3)	Fe(1)–C(4)	1.909(4)
Fe(1)–C(2)	1.944(3)	Fe(1)–C(3)	1.942(3)
Mn(1)–N(1)	2.258(3)	Mn(1)–N(2c)	2.209(3)
Mn(1)–O(1)	2.185(3)	C(1)–N(1)	1.151(4)
C(2)–N(2)	1.142(4)	C(3)–N(3)	1.144(4)
C(4)–N(4)	1.149(5)		
N(5)–Fe(1)–N(6)	82.08(11)	N(5)–Fe(1)–C(4)	93.97(13)
N(5)–Fe(1)–C(1)	174.96(12)	N(5)–Fe(1)–C(2)	93.88(12)
N(5)–Fe(1)–C(3)	87.45(12)	N(6)–Fe(1)–C(1)	96.49(13)
N(6)–Fe(1)–C(4)	175.42(13)	N(6)–Fe(1)–C(2)	88.64(12)
N(6)–Fe(1)–C(3)	90.43(12)	C(4)–Fe(1)–C(1)	87.67(15)
C(4)–Fe(1)–C(2)	89.33(14)	C(4)–Fe(1)–C(3)	91.71(14)
C(1)–Fe(1)–C(2)	90.91(13)	C(1)–Fe(1)–C(3)	87.73(13)
C(2)–Fe(1)–C(3)	178.26(14)	Fe(1)–C(1)–N(1)	176.3(3)
Fe(1)–C(2)–N(2)	177.0(3)	Fe(1)–C(3)–N(3)	177.5(3)
Fe(1)–C(4)–N(4)	177.3(3)	N(1)–Mn(1)–O(1)	92.87(11)
N(1)–Mn(1)–O(1a)	87.13(11)	N(1)–Mn(1)–N(2c)	89.61(11)
N(1)–Mn(1)–N(2h)	90.39(11)	O(1)–Mn(1)–N(2c)	89.97(13)
O(1)–Mn(1)–N(2h)	90.03(13)	Mn(1)–N(1)–C(1)	161.2(3)
Mn(1b)–N(2)–C(2)	160.7(3)		

Hydrogen Bonds

A	D	H	A...D	A...H–D
N(4)	O(3j)	H(6j)	2.868(1)	161.2(1)
O(2)	O(1)	H(2)	2.815(1)	169.5(1)
O(3)	O(1)	H(1)	2.711(1)	174.9(1)

^a Estimated standard deviations in the last significant digits are given in parentheses. ^b Symmetry code: (a) $-x, 1-y, -z$; (b) $1+x, y, z$; (c) $1-x, 1-y, -z$; (h) $-1+x, y, z$; (j) $1/2+x, 3/2-y, -1/2+z$.

Table 4. Selected Bond Lengths (Å) and Angles (deg)^{a,b} for **3**

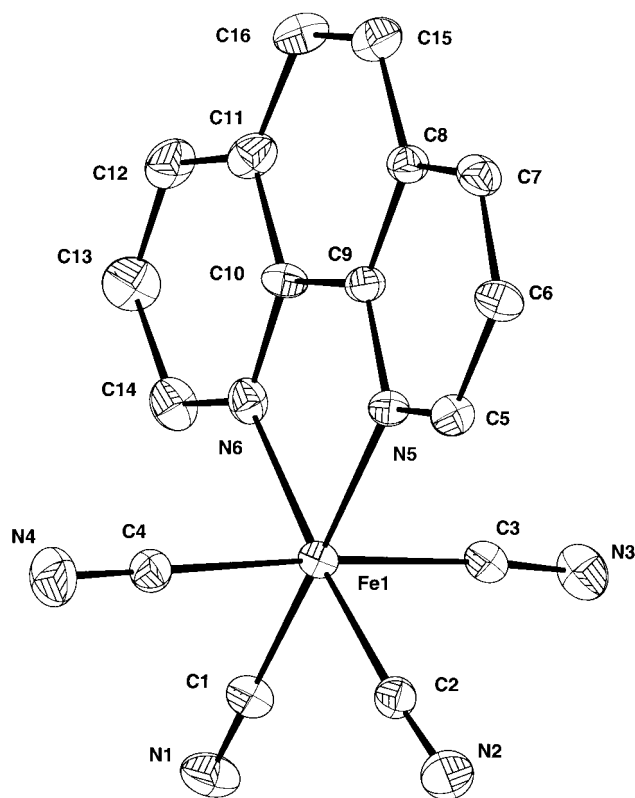
Fe(1)–N(5)	1.995(3)	Fe(1)–N(6)	1.992(3)
Fe(1)–C(1)	1.923(4)	Fe(1)–C(4)	1.910(4)
Fe(1)–C(2)	1.957(4)	Fe(1)–C(3)	1.949(4)
Zn(1)–N(1)	2.186(3)	Zn(1)–N(2c)	2.112(3)
Zn(1)–O(1)	2.105(3)	C(1)–N(1)	1.147(5)
C(2)–N(2)	1.131(5)	C(3)–N(3)	1.134(6)
C(4)–N(4)	1.145(5)		
N(5)–Fe(1)–N(6)	82.1(1)	N(5)–Fe(1)–C(4)	93.8(1)
N(5)–Fe(1)–C(1)	174.2(1)	N(5)–Fe(1)–C(2)	94.6(1)
N(5)–Fe(1)–C(3)	86.9(1)	N(6)–Fe(1)–C(1)	96.3(1)
N(6)–Fe(1)–C(4)	175.3(1)	N(6)–Fe(1)–C(2)	88.4(1)
N(6)–Fe(1)–C(3)	90.5(1)	C(4)–Fe(1)–C(1)	88.0(2)
C(4)–Fe(1)–C(2)	89.6(2)	C(4)–Fe(1)–C(3)	91.6(2)
C(1)–Fe(1)–C(2b)	90.9(2)	C(1)–Fe(1)–C(3)	87.6(2)
C(2)–Fe(1)–C(3)	178.0(1)	Fe(1)–C(1)–N(1)	175.1(3)
Fe(1)–C(2)–N(2)	175.9(3)	Fe(1)–C(3)–N(3)	177.7(4)
Fe(1)–C(4)–N(4)	176.7(4)	N(1)–Zn(1)–O(1)	92.2(1)
N(1)–Zn(1)–O(1a)	87.8(1)	N(1)–Zn(1)–N(2c)	89.4(1)
N(1)–Zn(1)–N(2h)	90.6(1)	O(1)–Zn(1)–N(2c)	89.1(1)
O(1)–Zn(1)–N(2h)	90.9(1)	Zn(1)–N(1)–C(1)	163.9(3)
Zn(1b)–N(2)–C(2)	163.9(3)		

Hydrogen Bonds

A	D	H	A...D	A...H–D
N(4)	O(3j)	H(6j)	2.885(5)	145.0(3)
O(2)	O(1)	H(2)	2.849(5)	170.4(2)
O(3)	O(1)	H(1)	2.726(5)	164.3(3)

^a Estimated standard deviations in the last significant digits are given in parentheses. ^b Symmetry code: (a) $-x, 1-y, -z$; (b) $1+x, y, z$; (c) $1-x, 1-y, -z$; (h) $-1+x, y, z$; (j) $1/2+x, 3/2-y, -1/2+z$.

ClO₄ (bpy = 2,2'-bipyridine) [1.928(7) and 1.931(7)]³¹ but also with those observed in the low-spin iron(II) complexes [Fe(phen)₂(CN)₂] [1.903(6) and 1.917(6) Å]²⁹ and K₂[Fe(bpy)-

**Figure 1.** Perspective drawing of the mononuclear [Fe(phen)(CN)₄][−] unit of complex **1** showing the atom numbering. Thermal ellipsoids are drawn at the 30% probability level.

(CN)₄·2.5H₂O [1.891(5)–1.936(5) Å].³² However, the presence of the tetraphenylphosphonium cation in the structure of **1** and the magnetic properties of this complex (see below) unambiguously reveal that **1** is a low-spin iron(III) complex. The same conclusion is obtained when looking at the position of the CN stretching frequency of the cyanide in **1** which appears as a medium intensity single peak at 2120 cm^{−1}. This value agrees well with that observed in the K₃[Fe(CN)₆] complex (2135 cm^{−1}) and it is clearly above those observed in the low-spin iron(II) species K₄[Fe(CN)₆] (2044 cm^{−1}) and [Fe(phen)₂(CN)₂] (2075 and 2062 cm^{−1}).

The rigid phenanthroline ligand is highly planar and the iron atom lies within this plane. Bond lengths and angles within the phen ligand are in agreement with those reported for the free phen molecule.³³ Although the separation between the mean planes of two phen ligands from adjacent [Fe(phen)(CN)₄][−] units is 3.5 Å, they are so slipped that no graphitic-like interaction may be considered (Figure 2). The bond lengths and angles involving the cyanide ligands are all normal [values of 1.15(1) and 1.14(1) Å] and they compare well with those found in the low-spin iron(III) complexes K₃[Fe(CN)₆] (1.131(23)–1.167(23) Å)³⁴ and [Fe(bpy)₂(CN)₂]ClO₄ (1.149(7)–1.151(7) Å).³¹ The iron atom and each cyanide are almost in a line [values for Fe–C–N ranging from 175.6(7)^o to 179.3(8)^o]. The bulky tetraphenylphosphonium cation exhibits the expected tetrahedral shape and its bond lengths and angles are as expected. Interestingly, the PPh₄⁺ cations are linked along the *c* axis by

(32) Nieuwenhuysen, M.; Bertram, B.; Gallagher, J. F.; Vos, J. G. *Acta Crystallogr.* **1998**, C54, 603.

(33) Nishigaki, S.; Yoshioka, H.; Nakatsu, K. *Acta Crystallogr., Sect. B* **1978**, 34, 875.

(34) Vannerberg, N. G. *Acta Chem. Scand.* **1972**, 26, 2863.

(31) Oshio, H.; Tamada, O.; Onodera, H.; Ito, T.; Ikoma, T.; Tero-Kubota, S. *Inorg. Chem.* **1999**, 38, 5686.

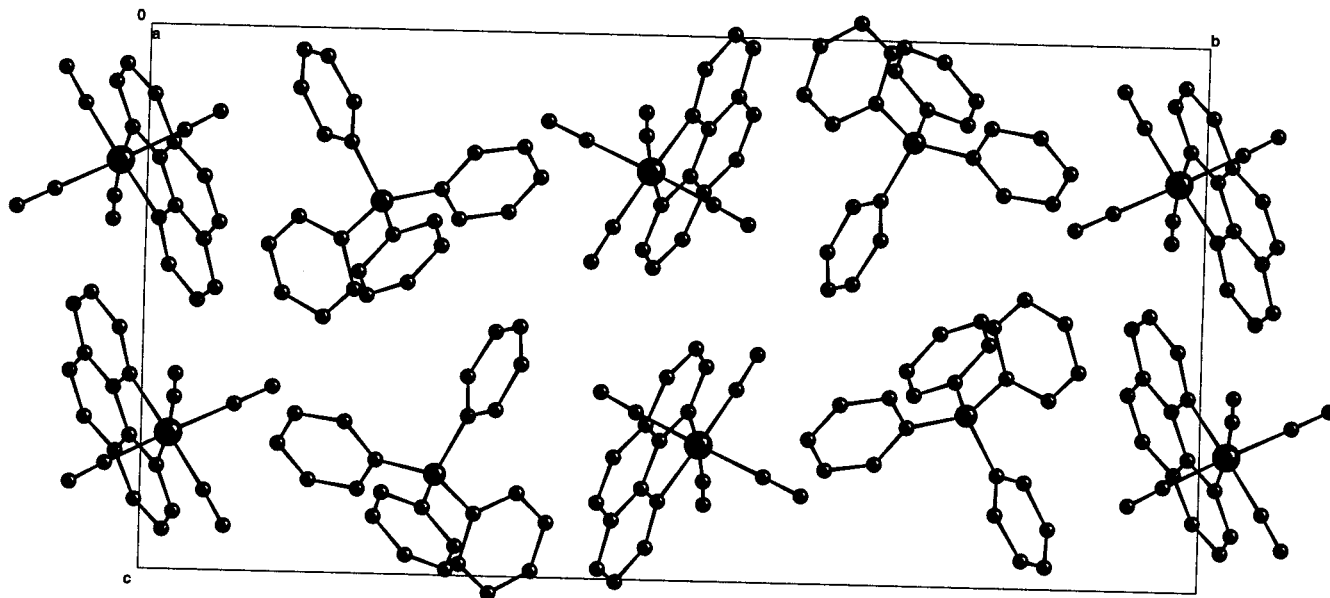


Figure 2. A projection of the crystal packing of **1** down the *x* axis. The water molecules have been omitted for clarity.

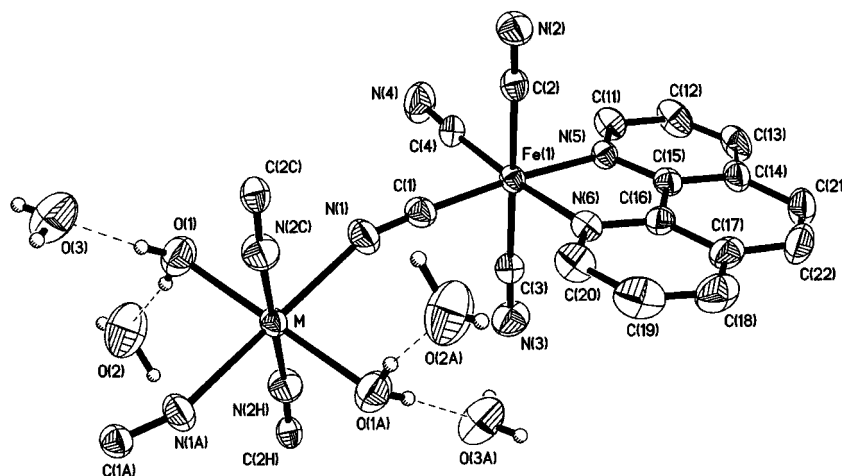


Figure 3. Perspective drawing of the asymmetric unit of complexes **2** (*M* = Mn) and **3** (*M* = Zn) showing the atom numbering. Thermal ellipsoids are drawn at the 50% (**2**) and 30% (**3**) probability levels. Hydrogen bonds involving the water molecules are illustrated by broken lines.

double phenyl embrace type interactions³⁵ (see Figure 2), two of the four phenyl rings of each cation being involved. The values of the mean intercentroid distance between the rings and the P···P separation are 3.43 and 7.32 Å, respectively.

Finally, two of the four cyanide groups and the water molecules are involved in hydrogen bond interactions with donor–acceptor distances N(1)···O(1a) [*a* = *x*, *-y* - 1/2, *z* - 1/2], N(3)···O(1b) [*b* = *-x*, *y* + 1/2, *-z* + 1/2] and O(1)···O(2) of 2.89(1), 2.84(1), and 2.65(1) Å, respectively. The shortest intermolecular iron–iron separation is 7.998(2) Å [Fe(1)···Fe(1d); (*d*) = 1 - *x*, 1 - *y*, 1 - *z*].

[{Fe(phen)(CN)₄}₂M(H₂O)₂]·4H₂O (*M* = Mn (**2**) and Zn (**3**)). Complexes **2** and **3** are isostructural compounds whose structure is made up of neutral double zigzag chains of formula [Fe(phen)(CN)₄]₂M(H₂O)₂ (*M* = Mn (**2**) and Zn (**3**)) and water molecules of crystallization which are linked by hydrogen bonds and van der Waals interactions. Within each chain, the [Fe(phen)(CN)₄]⁻ unit acts as a bismonodentate ligand toward M(H₂O)₂ units through two of its four cyanide groups in *cis* positions (Figure 3) affording bimetallic double chains contain-

ing Fe₂M₂ tetranuclear motifs which run parallel to the *a* axis (Figure 4). A view of the unit cell along the *a* axis (Figure 5) shows the parallel stacking of the phen ligands, the intrachain separation between the mean planes of two adjacent phen groups being 6.50 (**2**) and 6.35 Å (**3**).

As in **1**, each iron atom in **2** and **3** is coordinated by two phen nitrogen and four cyanide carbon atoms, taking a distorted octahedral geometry. The values of iron to phen nitrogen bond lengths (1.992(2)–1.995(3) Å in **2** and **3**) are slightly shorter and the angles subtended by the phen at the iron atom (82.08(11)^o (**2**) and 82.1(1)^o (**3**)) are somewhat larger than those found in **1**. The Fe(1)–C bond lengths in **2** (1.909(4)–1.944(3) Å) and **3** (1.910(4)–1.957(4) Å) are in good agreement with those observed in the low-spin iron(III) unit [Fe(phen)(CN)₄]⁻ of complex **1**. It deserves to be noted that the values of the two Fe–C bonds corresponding to the two *trans* coordinated cyano groups in **1**–**3** are significantly longer than those of the *cis* coordinated ones. The Fe(1)–C–N angles for both terminal (177.5(3)^o and 177.3(3)^o in **2** and 177.7(4)^o and 176.7(4)^o in **3**) and bridging (176.3(3)^o and 177.0(3)^o in **2** and 175.1(3)^o and 175.9(3)^o in **3**) cyanide groups depart somewhat from strict linearity. The manganese (**2**) and zinc (**3**) atoms are six

(35) Dance, I.; Scudder, M. *Chem.–Eur. J.* **1996**, *2*, 481.

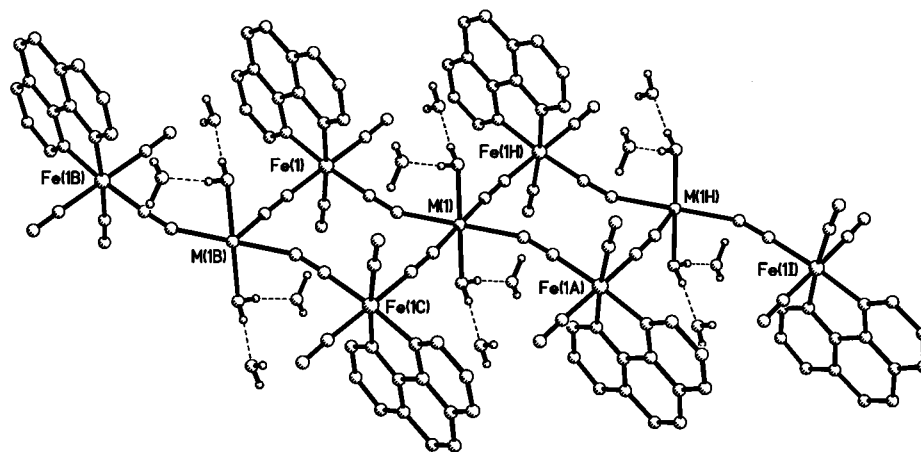


Figure 4. Perspective drawing of a fragment of the double zigzag chain of **2** ($M = \text{Mn}$) and **3** ($M = \text{Zn}$) running parallel to the a axis. Hydrogen bonds within the double zigzag chain are noted as broken lines.

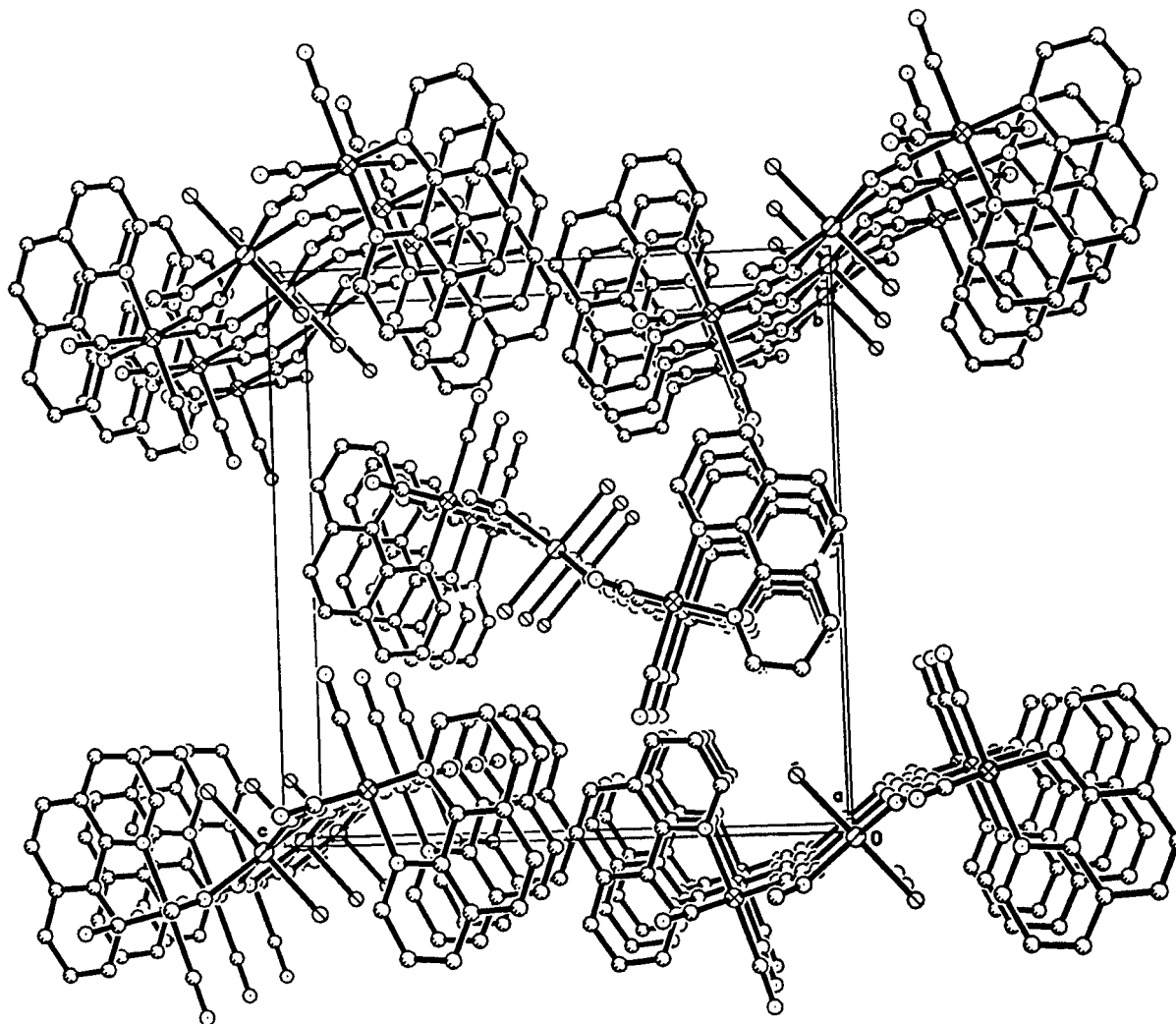


Figure 5. A view of the unit cell contents of **2** along the a axis showing the arrangement of the double chains.

coordinated: two water molecules in *trans* positions and four cyanide nitrogen atoms build a distorted octahedral surrounding around the metal atoms. The $M\text{--}O(w)$ bond lengths are 2.185(3) ($M = \text{Mn}$) and 2.105(3) Å ($M = \text{Zn}$), whereas the $M\text{--}N$ bond distances are 2.258(3) and 2.209(3) Å ($M = \text{Mn}$) and 2.186(3) and 2.112(3) Å ($M = \text{Zn}$). The shortening observed in this series of bonds when going from Mn to Zn is in agreement with the smaller ionic radius of Zn(II) vs Mn(II). The values of the

$M\text{--}N(1)\text{--}C(1)$ [$161.2(3)^\circ$ ($M = \text{Mn}$) and $163.9(3)^\circ$ ($M = \text{Zn}$)] and $M\text{--}N(2c)\text{--}C(2c)$ bond angles [$160.7(3)^\circ$ ($M = \text{Mn}$) and $163.9(3)^\circ$ ($M = \text{Zn}$)] exhibit significant deviations from linearity. The C–N bond lengths for terminal cyanide groups [1.144(4) and 1.149(5) Å (**2**) and 1.134(6) and 1.145(5) Å (**3**)] compare well with those observed in **1** and they are very close to the C–N bond distances for bridging cyanide ligands [1.151(4) and 1.142(4) Å (**2**) and 1.147(5) and 1.131(5) Å (**3**)].

The CN stretching region of the IR spectrum of **2** and **3** is consistent with the presence of bridging (two weak intensity peaks at 2170 and 2150 cm⁻¹) and terminal (a medium intensity and sharp absorption at 2125 cm⁻¹) cyanide ligands.

The values of the intrachain Fe(1)⋯M separation through bridging cyanide are 5.245(1) [Fe(1)⋯Mn(1)], 5.208(1) [Fe(1)⋯Mn(1b)], 5.187(1) [Fe(1)⋯Zn(1)], and 5.132(1) Å [Fe(1)⋯Zn(1b)]. These values which correspond to the edges of the Fe₂M₂ tetranuclear unit are much shorter than the metal–metal separations across its diagonals [7.251(1) (**2**) and 7.152(1) Å (**3**) for Fe(1)⋯Fe(1c) and 7.529(1) (**2**) and 7.440(1) Å (**3**) for M(1)⋯M(1h)]. The shortest interchain metal–metal separations are 8.572(1) (**2**) and 8.554(1) Å (**3**) [Fe(1)⋯Fe(1e); (e) = 1/2 - x, 1/2 + y, -1/2 - z], 7.615(1) (**2**) and 7.633(1) Å (**3**) [M(1)⋯Fe(1g); (g) = 1/2 - x, -1/2 + y, -1/2 - z] and 11.436(1) (**2**) and 11.388(1) Å (**3**) [M(1)⋯M(1f); (f) = 1/2 - x, 1/2 + y, 1/2 - z]. Finally, hydrogen bonds involving one of the terminal cyanide ligands and all the water molecules (see end of Tables 3 and 4) significantly contribute to stabilize the double zigzag chain motif of **2** and **3** (see Figure 4).

Magnetic Properties of 1–3. The temperature dependence of the $\chi_{\text{M}}T$ product for complex **1** (χ_{M} being the molar magnetic susceptibility) corresponds to a straight line: $\chi_{\text{M}}T$ monotonically decreases from 0.71 cm³ mol⁻¹ K at room temperature to 0.54 cm³ mol⁻¹ K at 1.9 K. The value of μ_{eff} (ca. 2.38 μ_{B}) at room temperature for **1** agrees with those previously reported for other low-spin iron(III) complexes³⁶ and it is significantly larger than the spin-only value for an isolated low-spin iron(III) center (0.375 cm³ mol⁻¹ K for $S = 1/2$ assuming $g_{\text{Fe}} = 2.0$). This result confirms the presence of a significant orbital contribution in **1**. The variation of $\chi_{\text{M}}T$ versus T for **1** is characteristic of a low-spin octahedral iron(III) system with spin–orbit coupling of the ²T_{2g} ground term.^{37–39} The significant distortion of the iron(III) environment in **1** (roughly C_{2v} symmetry around the metal atom) caused by the presence of one bidentate phen and four terminal cyanide ligands is not enough to quench totally the orbital contribution of the ground state. Our discussion of **1** is important because the same low-spin iron(III) complex is used as a ligand in **2** and **3**.

The temperature dependence of the $\chi_{\text{M}}T$ product for complex **2** (χ_{M} being the magnetic susceptibility per Fe₂Mn unit) is shown in Figure 6. The value of $\chi_{\text{M}}T$ at room temperature is 5.74 cm³ mol⁻¹ K. This value agrees with the presence of a high-spin Mn(II) and two low-spin Fe(III) magnetically isolated. As the temperature is lowered, the $\chi_{\text{M}}T$ product smoothly decreases, exhibits a pronounced minimum at 12.0 K ($\chi_{\text{M}}T$ being 2.60 cm³ mol⁻¹ K), and further increases sharply to reach a value of 26.0 cm³ mol⁻¹ K at 1.9 K. The magnetization curve of **2** at 2.0 K is shown in the insert of Figure 6. A value of 2.5 BM is attained at the maximum available magnetic field. No magnetic ordering is observed for **2** above 1.9 K according to *ac* and zero field cooled magnetization measurements.

The magnetic behavior of complex **3** (χ_{M} being the magnetic susceptibility per Fe₂Zn unit) is shown in Figure 7. $\chi_{\text{M}}T$ at room temperature for **3** is 1.39 cm³ mol⁻¹ K, a value expected for two magnetically isolated low-spin iron(III) (it is practically twice that of complex **1**). As the temperature is lowered, $\chi_{\text{M}}T$

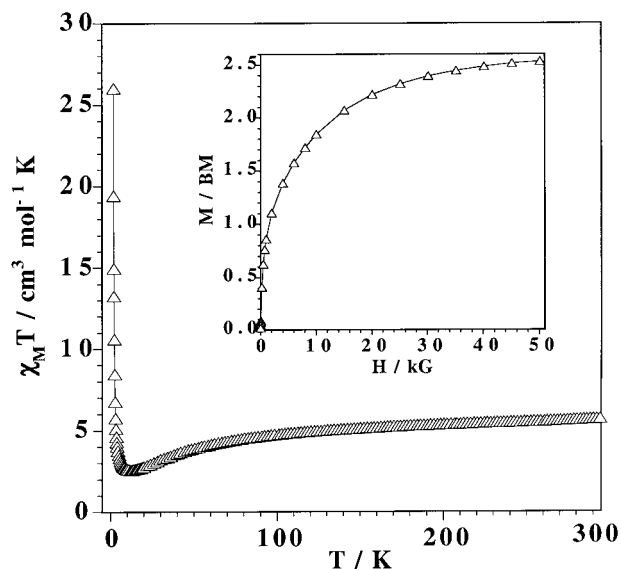


Figure 6. Thermal dependence of the $\chi_{\text{M}}T$ product for complex **2**: (Δ) experimental data; (—) eye-guide line. The insert shows the magnetization curve at 2.0 K.

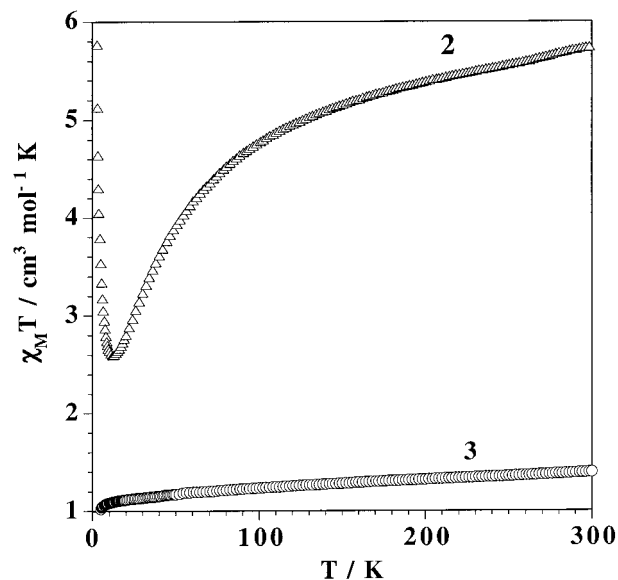


Figure 7. Thermal dependence of the $\chi_{\text{M}}T$ product for complex **3** (\circ). The magnetic data of complex **2** (Δ) are included for the sake of comparison.

of complex **3** smoothly decreases and reaches a value of 1.02 cm³ mol⁻¹ K at 1.9 K.

According to the double zigzag structure of compound **3**, its magnetic properties are due to the occurrence of two magnetically isolated low-spin iron(III) centers with significant spin–orbit coupling. The intrachain coupling between iron(III) centers separated by more than 10.2 Å through the –CN–Zn–CN–bridging skeleton in **3** is expected to be extremely small as shown by the similarity of the magnetic behaviors of complexes **1** and **3**. As far as the magnetic properties of **2** are concerned and in the lack of something better, a crude approximation of a “spin only” magnetic behavior for this compound can be obtained by subtracting from the $\chi_{\text{M}}T$ experimental curve twice the contribution of an isotropic low-spin iron(III) (experimental data for complex **1**). The resulting curve exhibits the same shape than that of complex **2**. This type of curve is typical of a ferrimagnetic behavior.^{40–42} The noncompensation between the antiferromagnetically coupled Mn(II) spin sextet and Fe(III) spin

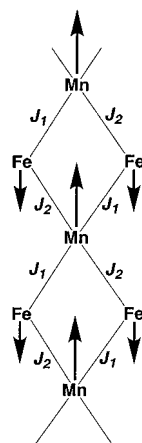
(36) Casey, A. T.; Mitra, S. In *Theory and Applications of Molecular Paramagnetism*; Boudreaux, E. A., Mulay, L. N., Eds.; John Wiley and Sons: New York, 1976; Chapter 3, p 191.

(37) Patra, A. K.; Ray, M.; Mukherjee, R. *Inorg. Chem.* **2000**, *39*, 652.

(38) Ray, M.; Mukherjee, R.; Richardson, J. F.; Buchanan, R. M. *J. Chem. Soc., Dalton Trans.* **1993**, 2451.

(39) Martin, L. L.; Martin, R. L.; Murray, K. S.; Sargeson, A. M. *Inorg. Chem.* **1990**, *29*, 1387.

Scheme 1



doublet across the cyanide bridges in **2** (see Scheme 1) accounts for this well documented magnetic behavior. The $t_{2g}-t_{2g}$ pathways ensure the antiferromagnetic coupling between the $t_{2g}^3e_g^2$ high-spin Mn(II) and $t_{2g}^5e_g^0$ low-spin Fe(III) involved in **2**. The lack of theoretical model to analyze the thermodynamic

(40) Verdagner, M.; Julve, M.; Michalowicz, A.; Kahn, O. *Inorg. Chem.* **1983**, *19*, 2624.

(41) (a) Verdagner, M.; Gleizes, A.; Renard, J. P.; Seiden, J. *Phys. Rev. B* **1984**, *29*, 5144. (b) Gleizes, A.; Verdagner, M. *J. Am. Chem. Soc.* **1984**, *105*, 3727.

(42) (a) Pei, Y.; Verdagner, M.; Kahn, O.; Sletten, J.; Renard, J. P. *Inorg. Chem.* **1987**, *26*, 138. (b) Kahn, O.; Pei, Y.; Verdagner, M.; Renard, J. P.; Sletten, J. *J. Am. Chem. Soc.* **1988**, *110*, 782.

properties of double-stranded ferrimagnetic chains precludes the modelization of the magnetic properties of **2** and thus to get an estimate of the value of the antiferromagnetic coupling in the Mn(II)–NC–Fe(III) pair. More experimental and theoretical work is needed to analyze properly the magnetic behavior of the double zigzag bimetallic chain **2** and the new spin topologies which can be expected by reacting the stable $[B^{III}(L)_x(CN)_y]^{(y-3)-}$ (L = polydentate ligand) mononuclear species with assembling complexes. The use of the organometallic $[Cp^*M(CN)_3]^-$ (M = Rh, Ir) species as a ligand toward coordinatively unsaturated metal complexes in a very recent report⁴³ illustrates the versatility and richness of the building block strategy in the preparation of cyano-bridged heterometallic species.

Acknowledgment. This work was supported by the TMR Program from the European Union (Contract ERBFMRXCT98-0181), the Spanish Dirección General de Investigación Científica y Técnica (DGICYT) (Projects PB97-1397 and PB98-1044), and Fundació Caixa Castelló-Bancaixa (Project PIB98-07). Thanks are also extended to the Servei Central d'Instrumentació Científica (SCIC) of the Universitat JAUME I for providing us with X-ray facilities.

Supporting Information Available: X-ray crystallographic files in CIF format for complexes **1–3**. This material is available free of charge via the Internet at <http://pubs.acs.org>.

IC001241A

(43) Contakes, S. M.; Klausmeyer, K. K.; Rauchfuss, T. B. *Inorg. Chem.* **2000**, *39*, 2069.